Journal of Cancer Research and Clinical Oncology (2019) 145:321–328
https://doi.org/10.1007/s00432-018-2786-2

ORIGINAL ARTICLE – CANCER RESEARCH

Glioma stem cells reconstruct similar immunoinflammatory microenvironment in different transplant sites and induce malignant transformation of tumor microenvironment cells

Tao Xie[1] · Bing Liu[1] · Chun-Gang Dai[1] · Zhao-Hui Lu[1] · Jun Dong[1] · Qiang Huang[1]

Received: 16 July 2018 / Accepted: 30 October 2018 / Published online: 10 November 2018

Abstract

Purpose This study aimed to examine whether the different tumor-transplanted sites could construct a similar immunoinflammatory microenvironment and to investigate the interactions between tumor microenvironment cells.

Methods The red fluorescent protein-SU3 (SU3-RFP) or SU3 glioma stem cells (GSC) were inoculated into the brain, liver, abdominal cavity, and subcutis of green fluorescent protein (GFP)-nude mice. The tumor tissues were taken to observe the tissue cell distribution. The single cell suspension of tumor tissues was prepared and cultured, while the SU3-RFP cells were co-cultured with the cells from GFP-transgenic mice. The RFP^+, GFP^+, and RFP^+/GFP^+ cells were traced by fluorescence microscope, and their protein expressions were determined by Western blot analysis. The markers of immunoinflammatory cells, including F4/80, CD11b, CD11c, CD80, CD47, and SIRP-α, were determined by RT-PCR and immunocytochemistry assays, respectively.

Results The xenograft models of all transplant sites were inducible, and the red tumor cells of tumor tissues were encircled by a great quantity of host-derived green cells, including immunoinflammatory cells with CD80, F4/80, CD11b, and CD11c expressions, which might generate the cell colonies and possess the pseudopodia. Additionally, the interactions between red tumor cells and green immunoinflammatory cells, including cell fusion process and yellow fusion cell formation, were observed in cultured cells. The fusion cells-derived B4 cells with expressions of CD47 and SIRP-α proteins had the strong proliferation ability and tumorigenic effect.

Conclusions The similar tumor immunoinflammatory microenvironment was constructed by GSC in different transplant sites, and the cell fusion indicated a malignant transformation of the tumor microenvironment cells.

Keywords Glioma stem cells · Transplantation tumor model · Tumor immunoinflammatory microenvironment · Malignant transformation of microenvironment cells

Abbreviations

GSC	Glioma stem cells
GFP	Green fluorescent protein
RFP	Red fluorescent protein
RT-PCR	Reverse transcription polymerase chain reaction
Sca-1	Stem/progenitor cell surface antigen-1

✉ Zhao-Hui Lu
luzhdoc@163.com

✉ Jun Dong
dongjun@suda.edu.cn

[1] The Experimental Center, Department of Neurosurgery, The Second Affiliated Hospital of Soochow University, 1055 Sanxiang Road, Suzhou 215004, Jiangsu, China

Introduction

Brain tumor microenvironment is composed of tumor cells, tumor stem cells, tumor vasculature, microglia/macrophages, astrocytes, and neural stem cells (Charles et al. 2011). These microenvironment components can cause the positive and negative effects on the growth of brain tumors. Among them, the microglia/macrophages, known as tumor-associated macrophages (Watters et al. 2005), may play an important role in the generation and development of brain tumors. Under normal physiological conditions, the macrophages, which reside in the brain, are called microglia (Hanisch and Kettenmann 2007) and remain constant despite small numbers. When the tumor occurs, the cells increase rapidly to play an immune surveillance role at the initial stage. However, they can also promote the growth of

tumors in the advanced stage (Bettinger et al. 2002). This functional conversion of the immunoinflammatory cells has aroused our intense interest, but its observation in the clinic is subject to the ethical limitation. In the present study, the red fluorescent protein (RFP)-transgenic human glioma stem cells (GSC) and green fluorescent protein (GFP)-transgenic nude mice, which may, respectively, present the tumor cells and immunoinflammatory microenvironment components in red and green, were used to investigate the interactions between these tumor microenvironment cells, especially in GSC and immunoinflammatory cells, which may be helpful for understanding the possible mechanisms of this transition.

Materials and methods

Materials

Human GSC SU3, RFP-transgenic SU3 (SU3-RFP), and GFP-transgenic BALB/c nude mice were prepared according to our previous methods (Wan et al. 2012; Zhu et al. 2013; Lu et al. 2014). Independent air supply cage system for raising animals was from Suzhou Suhang Technology Equipment Co., Ltd. (China). Fluorescence inverted microscope was from Nikon (Japan). CO_2 incubator was from Heraeus Company (Germany). The living cell workstation was from Olympus Company (Japan). Stereotaxic apparatus was from Huaibei Zhenghua Biological Equipment Co., Ltd. (China). Freezing microtome was from Leica Company (Germany). Animal brain slice mold was from Beijing Shuolinyuan Science and Technology Co., Ltd. (China). Anti-CD47, anti-SIRP-α, and anti-β-actin antibodies were provided by Abcam Company (England). Anti-RFP and anti-EGFP antibodies were provided by Biolegend Company (USA). DMEM medium and fetal bovine serum were provided by HyClone Corporation (USA).

Establishment of animal model

After being approved by the Ethical Committee of the Second Hospital Affiliated to Soochow University, GFP-transgenic BALB/c nude mice, weighing 20–22 g, were used for this study. These mice were housed in the specific pathogen-free cages in an independent air supply system. The care and use of the animals in the experiment conformed to the Clauses and General Recommendation of the Chinese Experimental Animal Administration Legislation in order to minimize the suffering and ensure the animal welfare. As required, the inoculated tumor cells might be SU3 or SU3-RFP, and the inoculated methods might be different according to the site of inoculation. For example, the brain inoculation in situ was achieved by slow injection of the tumor cells into the cranial cavity with stereotaxic apparatus, the subcutaneous inoculation was performed by injection of the tumor tissues with a medical trocar or injection of the tumor cells with a penicillin skin test syringe into the forelimb armpit or foot, the hepatic inoculation should be done that after incision of right rib margin, the tumor cells were then injected into the liver slowly through a micro-pump, and the peritoneal inoculation was a direct injection of the tumor cells into the abdominal cavity through the use of a syringe for penicillin skin test. Each nude mouse only accepted an inoculated method. The inoculated quantity of the tumor cells was determined according to the location of inoculation. The inoculation of the brain, liver, foot, armpit, and abdominal cavity required 10^5 cells/10 μl, 10^5 cells/15 μl, 10^6 cells/50 μl, 10^6 cells/100 μl, and 10^7 cells/100 μl normal saline, respectively. The animal number of each xenograft model was six nude mice.

Observation of tumor microenvironment

The partial tumor tissues were taken for frozen section and paraffin section to observe the tissue change and cell distribution under the white-light and fluorescence microscopes, respectively. To observe the tumor microenvironment cells, the fresh tumor tissues were collected, and the single cell suspension was prepared and cultured. For cell interaction study, the SU3-RFP cells were co-cultured with the trophoblast cells in the peritoneal lavage fluid or myeloid-derived suppressor cells in the bone marrow lavage fluid of GFP-transgenic mice. The RFP^+, GFP^+, and RFP^+/GFP^+ cells were traced dynamically under common and fluorescence inverted microscopes, the RFP^+/GFP^+ cells, namely yellow cells, were collected timely for monoclone and subculture according to our previous method (Wang et al. 2015). The each cellular experiment was repeated three times.

Measurement of mRNA expression

The expressions of CD1a, CD11b, CD11c, CD68, CD80, CD83, CD86, F4/80, RFP, EGFP, and β-actin mRNA in the cultured cells were determined by reverse transcription polymerase chain reaction (RT-PCR) method as described previously (Wang et al. 2013). The amplified PCR products were separated on a 1.5% agarose gel. The β-actin was used as an internal control in the experiment.

Measurement of protein expression

The expressions of RFP, GFP, and β-actin proteins in cultured cells were determined by Western blot method as described previously (Zhao et al. 2014). In a typical procedure, an aliquot of 50 μg protein from each sample was separated on 10% SDS–polyacrylamide gel by electrophoresis and then transferred to nitrocellulose membranes. The

membranes were, respectively, incubated with different primary antibodies overnight at 4 °C and then incubated with fluorescent secondary antibody at room temperature for 1 h. Finally, the protein bands were photographed. The expressions of CD47 and SIRP-α proteins in cultured cells were determined according to previous immunohistochemistry method (Chen et al. 2011).

Statistical analysis

The quantitative data were expressed as means ± standard deviation (SD), and the statistic difference between groups was determined by two-way analysis of variance (ANOVA) followed by a post hoc least significant difference test. The statistical analysis was conducted using SPSS 19.0 software (IBM, USA), $P < 0.05$ was considered statistically significant.

Results

RFP/GFP-traced tumor tissues

The hematoxylin and eosin staining observation under a light microscope showed that tumor cells of all transplant sites were distributed densely in the tumor tissues, with hyperchromatic nuclei, and accompanied with other common phenotypes of malignant tumor such as rich vascularity and necrotizing hemorrhage (Fig. 1b, e, h, k, l). However, it was difficult to distinguish between the interstitial components and the tumor cells. Under a fluorescence excitation, the tumor cells indicated a red appearance (Fig. 1a, c, f, g), while the host-derived cells, including immunoinflammatory cells from GFP-transgenic nude mice, were present in a green (Fig. 1a, c, f, g, i).

GFP-traced tumor immunoinflammatory microenvironment

Almost all organs, tissues, and cells of the GFP-transgenic nude mice were characterized by green appearance except that in the hair and red blood cells. As shown in Fig. 2 upper two rows, the host-derived tumor tissues and cellular microenvironment in the transplant brain tumors were present in a green under a fluorescence microscope, which was obviously different from the red tumor cells. Generally, the hematoxylin and eosin staining observation may determine the tumor microenvironment location, and the subsequent fluorescence excitation may observe the green components in the microenvironment in the same field of view. In such a situation, we observed that some tumor cells were encircled by a great quantity of green cells (Fig. 2a, b) and there were numerous green cells in the tumor necrosis foci (Fig. 2c–e). A number of green cells were also seen in the tumor edema reaction zone at the margin of the tumor (Fig. 2f) and in the larger host vessels (Fig. 2g–i). To identify whether the above these green cells contained the immunoinflammatory cells, the single cell suspension of tumor tissues was prepared and cultured in vitro. The results revealed that some green cells might generate the cell colonies (Fig. 2j, k) and possess the typical pseudopodia (Fig. 2l). The latter indicated a characteristic of macrophages or dendritic cells. The further RT-PCR assay showed that the markers of immunoinflammatory cells, including F4/80, CD11b, CD11c, and CD80, were highly expressed in the cells (Fig. 2m).

Cell fusion between GSC and immunoinflammatory cells

The SU3-RFP inoculations of liver and abdominal cavity could result in the cancerous ascites in some extent, especially in the advanced stage of the tumor. After the ascites was cultured in vitro, the smear examination observed that under a fluorescent microscope, the most of cells were identified as the green cells except for a few red tumor cells that have fallen off the solid tumor (Fig. 3d). Interestingly, a phagocytic reaction of the biggish green cells occurred targeting the red cells (Fig. 3e), and the red cells could also engulf the green cells (Fig. 3f). Importantly, some of these cells might change to the binuclear cells (Fig. 3g–j), which might be the fusion cells of GSC with immunoinflammatory cells. However, the cell fusion might be a transient phenomenon and not completely certain. So, the SU3-RFP cells were further co-cultured with the cells from peritoneal lavage liquid of GFP-transgenic mice, the cells of our interest were traced and observed in the living cells workstation by using lapse photography. The results showed that the yellow fusion cells could also occur in the co-cultured cell populations, and the fusion time was about 170 min from two monocytes to a binucleate cell (Fig. 3k, l) and subsequent 140 min from two nuclei to one nucleus (Fig. 3m). Additionally, we also observed that a binucleate cell might divide into two monocytes and the time was about 1260 min (Fig. 3n–q). To further determine whether the yellow fusion cells might co-express the RFP and GFP markers, the RT-PCR (Fig. 3a, b) and Western blot (Fig. 3c) assays were used. The results showed that the yellow fusion cells-derived B4 cells could express the RFP, GFP, and markers of inflammatory cells, the latter included the CD1a, CD83, and CD86.

The cancerous phenotype of fusion cells

On day four after cell culture, we observed that the proliferation of fusion cells-derived B4 cells was faster than that of host-derived malignant transformation cells B9 and B10 cells or SU3-RFP cells (Fig. 4a, $P < 0.01$), which might be

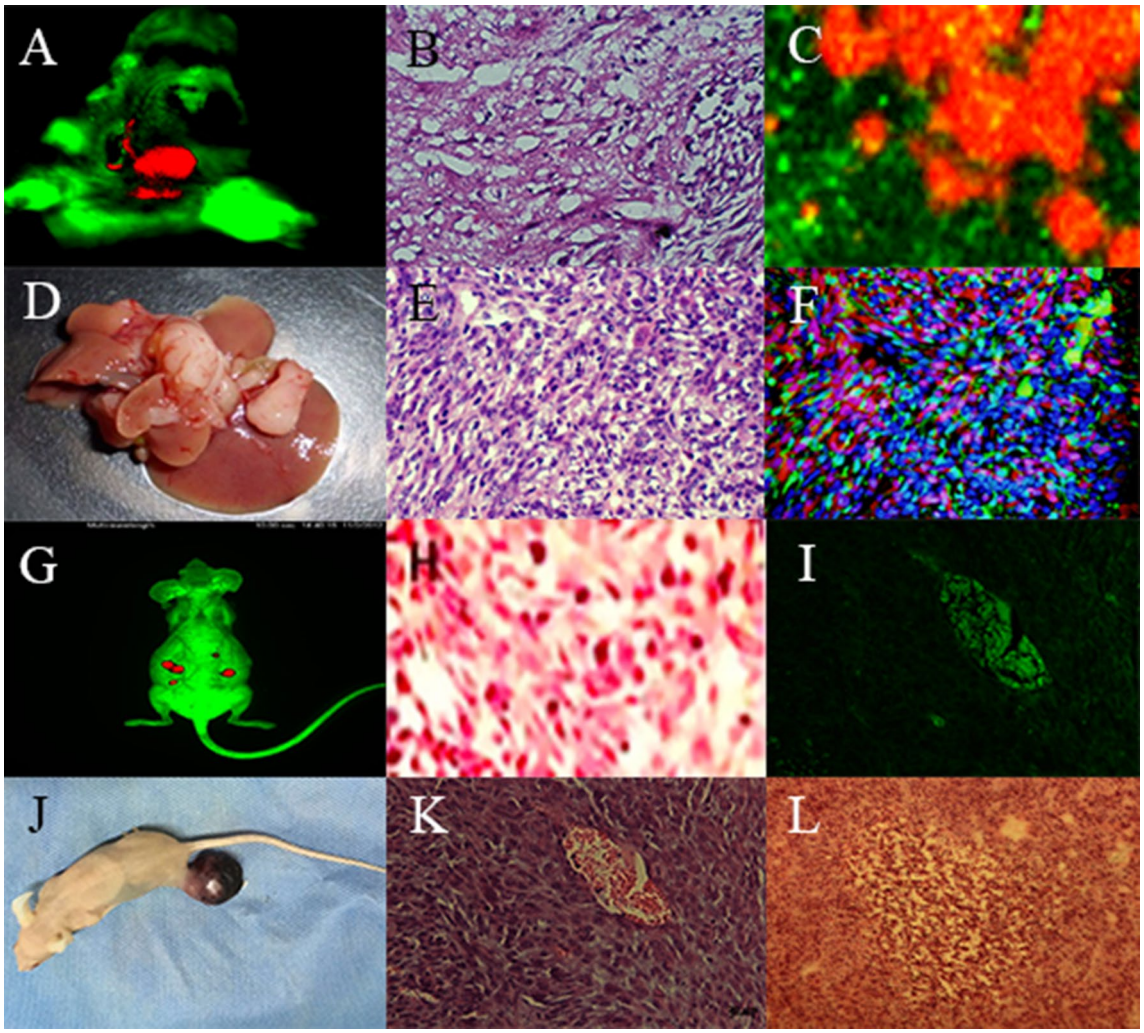

Fig. 1 The basic characteristics of tumor microenvironment in different transplant sites. The SU3-RFP in the brain **a** and abdominal cavity **g** could clearly show the size and location of the tumors (red) on the multifunctional living imaging system. In the tissue sections of hematoxylin and eosin staining, the tumor cells under a white-light microscope were characterized by malignant phenotypes of deep staining, irregular shape, and compact arrangement in the transplant tissues, including brain (**b**, original magnification 100×), liver (**e**, original magnification 100×), abdominal cavity (**h**, original magnification 200×), foot (**k**, original magnification 100×), and forelimb armpit (**l**, original magnification 40×). Under a fluorescence microscope, the red tumor cells (**c**, **f**, original magnification 100×), green host cells (**c**, **f**), and nucleated blood cells (**i**, original magnification 100×) were seen in the same horizon above the same section. The photo of **d** was the transplanted tumor in the liver, and that of **j** was the nude mice with transplanted tumor in the foot

identified as a malignant transformation of the tumor immunoinflammatory microenvironment cells in terms of tumorigenic rate (6/6) (Fig. 4b), histological changes of transplant tumors (Fig. 4c), and expressions of CD47 and SIRP-1α proteins (Fig. 4d, e).

Discussion

Several xenograft models of human GSC in GFP-transgenic nude mice have been reported by our previous research (Dong et al. 2010, 2011, 2012; Dai et al. 2015; Shen et al. 2015; Sun et al. 2015). In the present study, the SU3-RFP cells were transplanted into the GFP-transgenic nude mice, and the xenograft models with dual-color fluorescence tracing were established to observe the histological changes of tumor tissues and interactions between tumor microenvironment cells. Under a fluorescent microscope, all the green components, including cells and amorphous products in the tumor tissues, should be identified as host-derived tumor microenvironment components. The main advantage of the dual-color fluorescence tracing method not only achieves a clear distinguish of cells with two different colors, but also reflects the relationship among tumor angiogenesis, invasion, dissemination, necrosis focus repair, and the cell location of the tumor response zone, no matter in vivo imaging

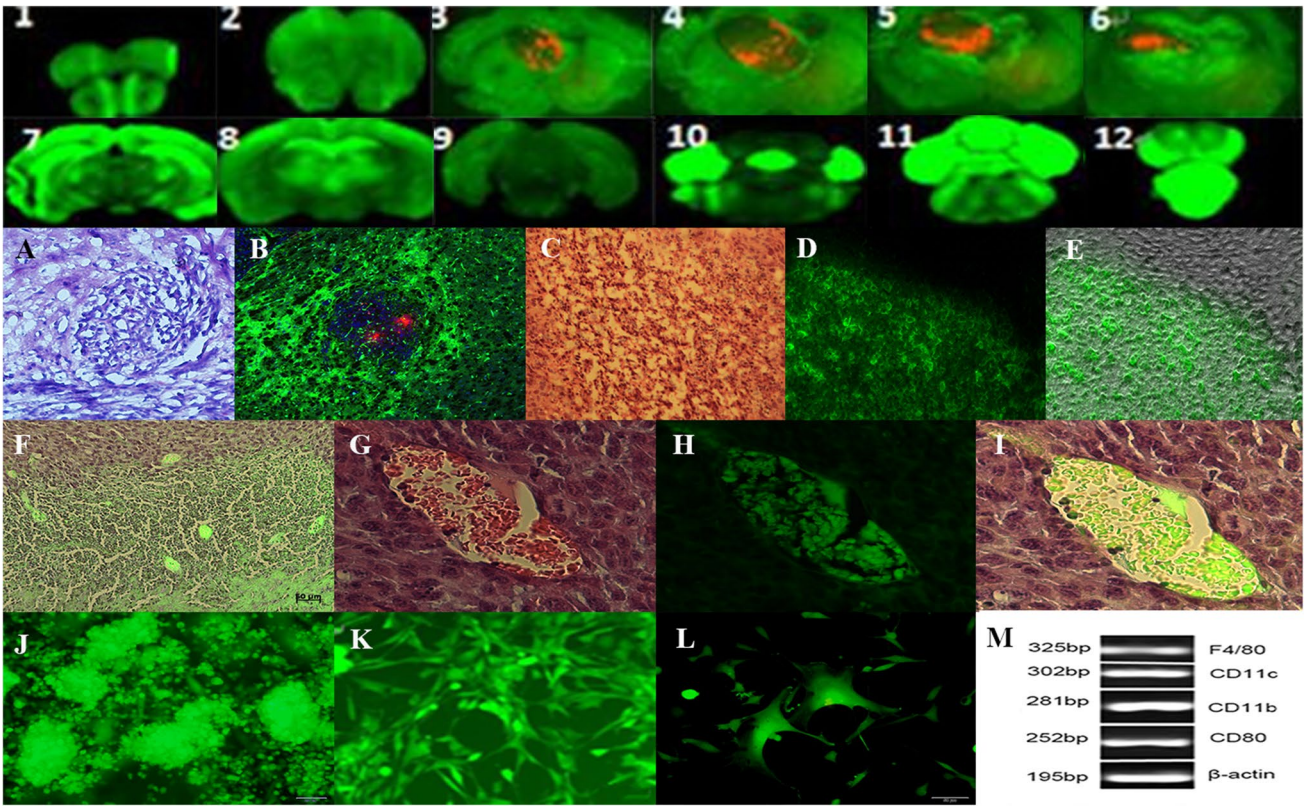

Fig. 2 The immunoinflammatory microenvironment of transplant tumors. Upper row 1–12 (original magnification 10×) showed the results of transplant brain tumor sections under a fluorescence microscope, the red tumors were seen and distinguished from a green microenvironment (3–6). A large number of small round green cells were observed in the tumor foci (**a**, original magnification 100×; **b**, original magnification 40×), tumor necrosis foci (**c**–**e**, original magnification 100×), tumor margin (**f**, original magnification 100×), and tumor vessel (**g**–**i**, original magnification 200×) under the white-light (**a, c**, **g**) and fluorescence (**b, d, e, f, h**, **i**) microscopes, respectively. These cultured green cells had certain colony forming ability (**j**, original magnification 100×), which was predominated by polygon (**k**, original magnification 200×) in morphology, including dendritic change (**l**, original magnification 400×). The markers of inflammatory cell related molecules were determined by RT-PCR assay (**m**)

or living-cell imaging, and in tissue sections or cell smears (Lu et al. 2014; Shen et al. 2015; Sun et al. 2015). The present results showed that the tumorigenesis of inoculated sites and dual-color fluorescences of inoculated tissues were observed in all animal models, suggesting that the growth sites of the transplanted tumors were not limited.

Some literature data have shown that bone marrow-derived cells are able to undergo the physiological fusion with somatic cells (Alvarez-Dolado et al. 2003; Duelli and Lazebnik 2007). Subsequently, a hypothesis was proposed by Dittmar et al. (2011), and they thought that the cell fusion might be the cause of carcinogenesis, no less important than cancer stem cells as the starting cells for cancer, which was also supported by some researchers (Lu and Kang 2011). However, it must be noted that physiological and pathological fusions should be distinguished since the fusion cells observed in tumor tissues were not unique to tumors. The incidence of the tumor cell fusion is only about 1% (Lu and Kang 2009), and it is difficult to identify the fusion cells by conventional sectioning. In 1974, some researchers believed that the binuclear and multinucleate giant cells observed in the pathological section of tumor tissues were the fusion cells (Sheehy et al. 1974), which, however, should not be of primary evidence. In our present study, the observation of cell fusion process was very intuitive by using dual-color fluorescence tracing technology, especially for RFP/GFP dual-positive yellow cells. But the yellow cells might be not the fusion cells due to an entosis appearance in some tumor cells (Overholtzer et al. 2007), which might be understood as a non-apoptotic cell death mode and an outcome of a cell entering into another cell. It is important to note that all such fusion cells, like real fusion cells, might also express the two kinds of fluorescence. Therefore, only the yellow cells that possessed a potential to two new viable cells and no exocytosis were identified as the fusion cells. In this study, the detected fusion cells were sequentially traced to exclude the entosis. The present results observed that the fusion time from two monocytes to a binucleate cell was about

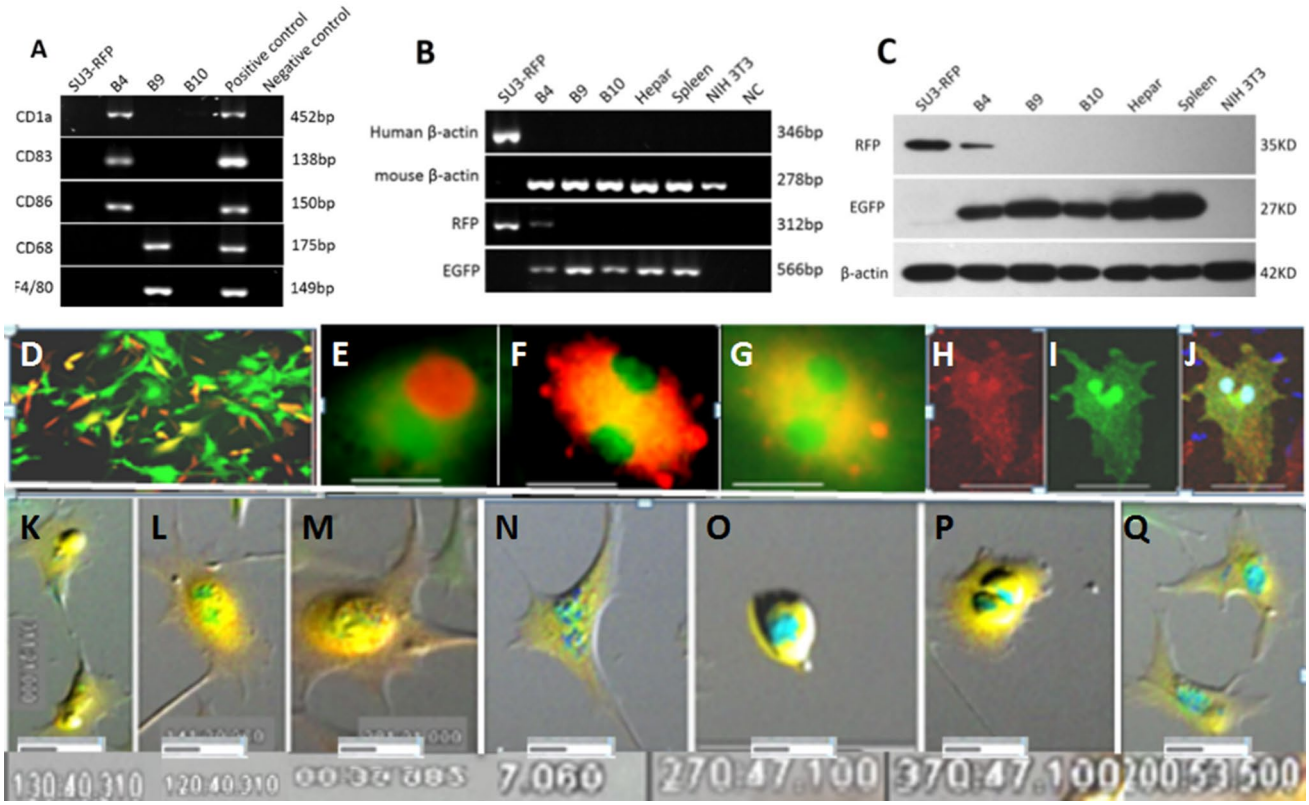

Fig. 3 The fusion between tumor cells and immunoinflammatory cells. **a** The mRNA expressions of CD1a, CD83, and CD86 in B4 cells and of CD68 and F4/80 in B9 cells, which was detected by RT-PCR method. **b, c** The results of RFP/GFP co-expressed B4 cells and GFP-expressed B9 and B10 cells using RT-PCR and Western blot methods, respectively. **d** The cultured cell populations of ascites from SU3-RFP-inoculated liver mice, and the B4 cells were obtained from the yellow cells by monoclonal screening. **e–j** The results of B4 cells under a phase contrast fluorescence microscope (50 μm) and exhibited a green cell engulfed a red cell **e**, a red cell engulfed two green cells **f**, a binuclear yellow cell **g**, and a binuclear fusion cell displayed by red **h**, green **i**, and Merge **j**, respectively. **k–q** The photos by lapse photography in the living cells workstation (200 μm). By sentinel tracking observation, as shown in **k–m**, the fusion time from two monocytes **k** to a binucleate cell **l** was about 170 min, and two nuclei fused into one nucleus took appropriate 140 min **m**. As illustrated in **n–q**, the time from a binucleate cell entering into the mitotic prophase **o**, mitotic phase **p**, and final two monocyte formation **q** was 1260 min in total

170 min and from two nuclei to one nucleus took appropriate 140 min, while the time from a fusion cell division into two new monocytes was 1260 min. Importantly, the process of the cell fusion might be not limited to the cytoplasm of two cells, and that the nucleus changes. The latter may be categorized into the heterokaryon and synkaryon. In the current experiment, we observed the synkaryon, which took about 140 min to become a heterozygote with one nucleus.

Recently, the cell fusion hypothesis of the cancer stem cells was proposed by Lu and Kang (2011). According to this hypothesis, the original fusion cells may be from the local tissue stem cells, differentiated cells, disseminated cells, and bone marrow-derived stem cells/non-stem cells. The fusion cells of our observation in this study were not belonging to any of the above, and it might be a new model, which was the fusion of SU3 GSC with host-derived immunoinflammatory cells. Even immunoinflammatory cells were differentiated cells when fusion, the fused cells might be reshaped into the cancer stem cells. Pawelek observed that the reshaped cancer stem cells might be different from the parental cancer stem cells (Pawelek 2005). The present results showed that the proliferation rate was faster in the fusion cells-derived B4 cells than in the parental SU3 cells, indicating a higher degree of malignancy. We also observed the high expressions of CD47 and SIRP-α proteins in the B4 cells, suggesting that the malignant cancer cells might originate from macrophages or dendritic cells. The potential reason might be that these cancer cells could up-regulate the expression of CD47, which might antagonize the phagocytosis by interacting with the SIRP-a on the surface of myeloma associated macrophages (Kim et al. 2012). Therefore, we believed that there was a new sort of cancer stem cells, which might be attributable to the symbiosis of tumor cells with microenvironment cells, but the exact interactions between them are necessary to research further. Also, we did not investigate the inflammation-related cytokines in the

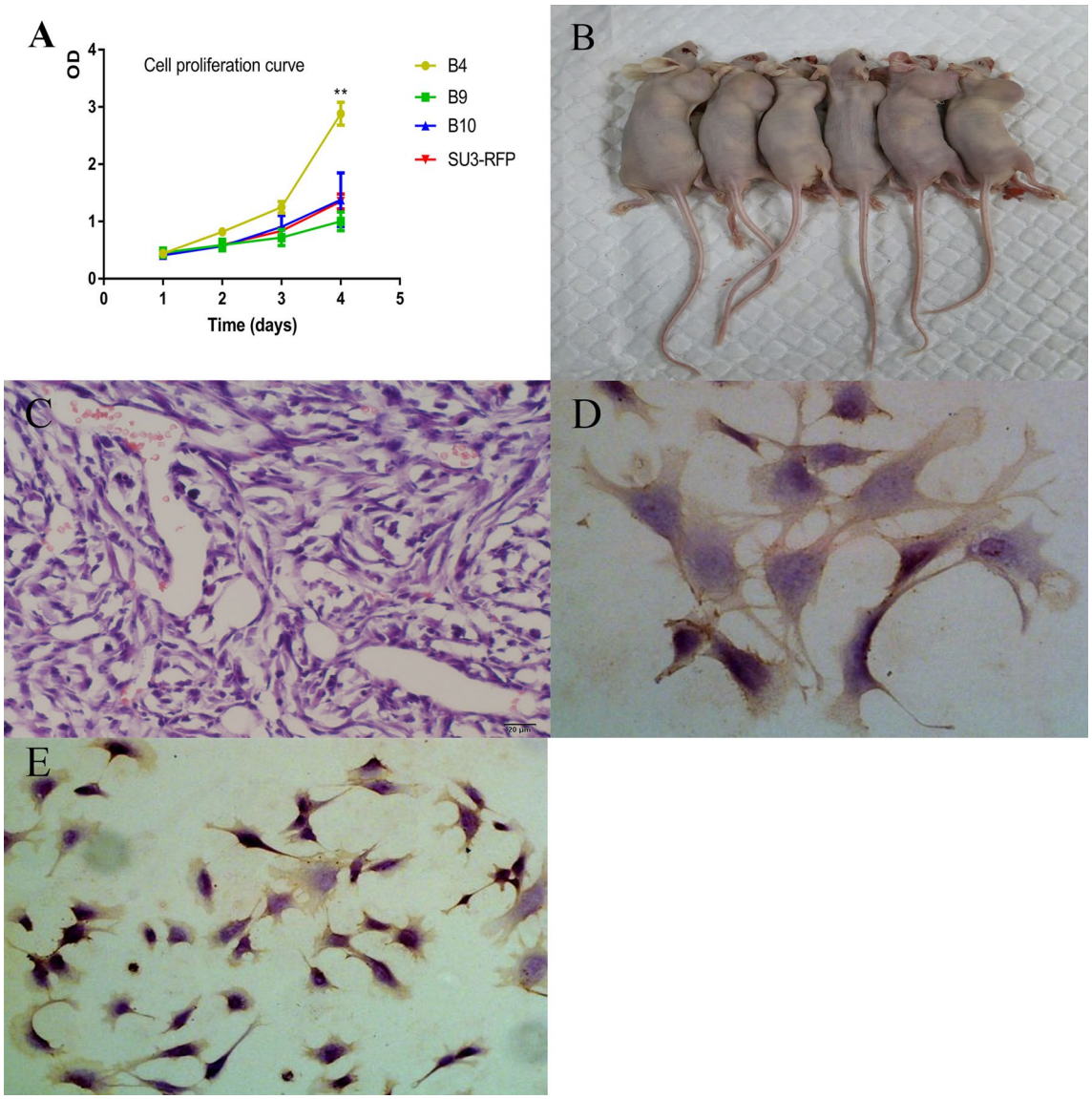

Fig. 4 The cancerous phenotype of fusion cells. **a** The cell proliferation curve, the proliferation of B4 cells (at the top) was faster than that of host malignant transformation cells-derived B9 and B10 or SU3-RFP cells. (Each value represents the means ± SD, with $n = 6$ per group. $^{**}P < 0.01$ versus SU3-RFP, B9 or B10 cells.) **b, c** B4 cells-induced tumor in nude mice and its slice, which exhibited the tumor size 35 days after transplantation **b** and the histological changes under a white-light microscope (**c**, original magnification 200×). **d** (original magnification 400×) and **e** (original magnification 200×) were the results of immunocytochemical staining for CD47 and SIRP-α in cultured B4 cells, respectively, the deep brown immune complex was observed in the cytoplasm

tumor microenvironment, which was a deficiency and will be needed to clarify the issue. However, our present results demonstrated a malignant transformation of the tumor microenvironment cells, which might be associated with the occurrence of tumor drug resistance (Sun et al. 2016; Zheng et al. 2018).

In conclusion, our present study demonstrated that the similar tumor immunoinflammatory microenvironment could be constructed by SU3 GSC in different transplant sites, and the cell fusion in the tumor microenvironment might indicate a malignant transformation of the tumor microenvironment cells. These findings may be helpful for understanding some features of the tumor immunoinflammatory microenvironment and drug resistance of the malignant glioma.

Acknowledgements This work was supported by the National Natural Science Foundation of China (no. 81472739), Science & Technology Project for Medical Health of Suzhou New District (no. 2017Q011), and Suzhou Science & Technology Development Project (no. SYS201507).

Compliance with ethical standards

Conflict of interest The authors declare no conflict of interest.

Ethical approval All procedures performed in studies involving animals were in accordance with the ethical standards of the institution or practice at which the studies were conducted.

Informed consent Informed consent was obtained from all individual participants included in the study.

References

Alvarez-Dolado M, Pardal R, Garcia-Verdugo JM et al (2003) Fusion of bone-marrow-derived cells with Purkinje neurons, cardiomyocytes and hepatocytes. Nature 425:968–973

Bettinger I, Thanos S, Paulus W (2002) Microglia promote glioma migration. Acta Neuropathol 103:351–355

Charles NA, Holland EC, Gilbertson R, Glass R, Kettenmann H (2011) The brain tumor microenvironment. Glia 59:1169–1180

Chen R, Xue J, Xie ML (2011) Reduction of isoprenaline induced myocardial TGF-β1 expression and fibrosis in osthole-treated mice. Toxicol Appl Pharmacol 256:168–173

Dai X, Chen H, Chen Y et al (2015) Malignant transformation of host stromal fibroblasts derived from the bone marrow traced in a dual-color fluorescence xenograft tumor model. Oncol Rep 34:2997–3006

Dittmar T, Schwitalla S, Seidel J et al (2011) Characterization of hybrid cells derived from spontaneous fusion events between breast epithelial cells exhibiting stem-like characteristics and breast cancer cells. Clin Exp Metastasis 28:75–90

Dong J, Zhang QB, Huang Q et al (2010) Glioma stem cells involved in tumor tissue remodeling in a xenograft model. J Neurosurg 113:249–260

Dong J, Zhao YD, Huang Q et al (2011) Glioma stem/progenitor cells contribute to neovascularization via transdifferentiation. Stem Cell Rev Rep 7:141–152

Dong J, Dai XL, Lu ZH et al (2012) Incubation and application of transgenic green fluorescent nude mice in visualization studies on glioma tissue remodeling. Chin Med J 125:4349–4354

Duelli D, Lazebnik Y (2007) Cell-to-cell fusion as a link between viruses and cancer. Nat Rev Cancer 7:968–976

Hanisch UK, Kettenmann H (2007) Microglia: active sensor and versatile effector cells in the normal and pathologic brain. Nat Neurosci 10:1387–1394

Kim D, Wang J, Willingham SB, Martin R, Wernig G, Weissman IL (2012) Anti-CD47 antibodies promote phagocytosis and inhibit the growth of human myeloma cells. Leukemia 26:2538–2545

Lu X, Kang YB (2009) Cell fusion as a hidden force in tumor progression. Cancer Res 69:8536–8539

Lu X, Kang YB (2011) Cell fusion hypothesis of the cancer stem cell. Adv Exp Med Biol 714:129–140

Lu ZH, Lv K, Zhang JS et al (2014) Establishment of a green fluorescent protein tracing murine model focused on the functions of host components in necrosis repair and the niche of subcutaneously implanted glioma. Oncol Rep 31:657–664

Overholtzer M, Mailleux AA, Mouneimneet G et al (2007) A nonapoptotic cell death process, entosis, that occurs by cell-in-cell invasion. Cell 131:966–979

Pawelek JM (2005) Tumour-cell fusion as a source of myeloid traits in cancer. Lancet Oncol 6:988–993

Sheehy PF, Wakonigv T, Winn R, Clarkson BD (1974) Asynchronous DNA synthesis and asynchronous mitosis in multinuclear ovarian cancer cells. Cancer Res 34:991–996

Shen YT, Zhang QB, Zhang JS et al (2015) Advantages of a dual-color fluorescence-tracing glioma. orthotopic implantation model: detecting tumor location, angiogenesis, cellular fusion and the tumor microenvironment. Exp Ther Med 10:2047–2054

Sun C, Zhao DL, Dai XL et al (2015) Fusion of cancer stem cells and mesenchymal stem cells contributes to glioma neovascularization. Oncol Rep 34:2022–2030

Sun X, Bao J, Shao Y (2016) Mathematical modeling of therapy-induced cancer drug resistance: connecting cancer mechanisms to population survival rates. Sci Rep 6:22498

Wan Y, Fei XF, Wang ZM et al (2012) Expression of miR-125b in the new, highly invasive glioma stem cell and progenitor cell line SU3. Chin J Cancer 31:207–214

Wang XY, Xue J, Yang J, Xie ML (2013) Timed high-fat diet in the evening affects the hepatic circadian clock and PPARα-mediated lipogenic gene expressions in mice. Genes Nutr 8:457–463

Wang AD, Dai XL, Cui BQ et al (2015) Experimental research of host macrophage canceration induced by glioma stem progenitor cells. Mol Med Rep 11:2435–2442

Watters JJ, Schartner JM, Badie B (2005) Microglia function in brain tumors. J Neurosci Res 81:447–455

Zhao X, Xue J, Wang XL, Zhang Y, Deng M, Xie ML (2014) Involvement of hepatic peroxisome proliferator-activated receptor α/γ in the therapeutic effect of osthole on high-fat and high-sucrose-induced steatohepatitis in rats. Int Immunopharmacol 22:176–181

Zheng Y, Bao J, Zhao Q, Zhou T, Sun X (2018) A spatio-temporal model of macrophage-mediated drug resistance in glioma immunotherapy. Mol Cancer Ther 17:814–824

Zhu YD, Dai XL, Zhao DL, Sun C, Dong J, Huang Q (2013) The effect of glioma stem/progenitor cell on tumor angiogenesis traced by red/green fluorescent protein. Chin J Exp Surg 30:297–299